



Bone marrow mesenchymal stem cells-derived exosomal miR-185-5p plays a protective role in high-glucose stimulated human retinal microvascular endothelial cells in vitro by regulating CXCL8

Lin Zhou*, Weixia Wang

Department of Ophthalmology, Huai'an Second People's Hospital (The affiliated Hospital of Xuzhou Medical University), Huaian, Jiangsu 223002, China

ARTICLE INFO

Original paper

Article history:

Received: August 27, 2023

Accepted: December 25, 2023

Published: December 31, 2023

Keywords:

CXCL8, diabetic retinopathy, bone marrow mesenchymal stem cells, exosomes, inflammatory factors

ABSTRACT

In this study, we intended to probe the impacts and mechanism of bone marrow mesenchymal stem cells (BM-MSCs)-derived exosomal miR-185-5p on angiogenesis and inflammatory response in diabetic retinopathy (DR). Based on the GEO database, we found that CXCL8 was differentially expressed in DR, and GO and KEGG analysis further revealed that CXCL8 was associated with angiogenesis and inflammatory response. Upstream miR-185-5p of CXCL8 was predicted by bioinformatics analyses and the binding relation between miR-185-5p and CXCL8 was further validated by dual-luciferase reporter assay. Human retinal microvascular endothelial cells (HRMECs) were added with high-glucose (HG) to construct a DR cell model. Exosomes secreted by BM-MSCs were isolated, and the DR cell model was treated with different intervention vectors of exosomes. Cell proliferation and angiogenesis were measured by MTT assay and Matrigel angiogenesis experiment, respectively, and the levels of VEGF, TNF- α , IL-1 β as well as IL-6 were examined by ELISA. The results showed that CXCL8 was highly expressed in HRMECs treated with HG. CXCL8 knockdown inhibited the proliferation, angiogenesis as well as concentration of inflammatory factors in DR cell models, while overexpression of CXCL8 had the opposite effects. CXCL8 was verified to be directly targeted by miR-185-5p. BM-MSCs-derived exosomes inhibited the proliferation, angiogenesis and concentration of inflammatory factors of DR cell models, but this effect was partly reversed by miR-185-5p inhibitor. In conclusion, BM-MSCs-derived exosomal miR-185-5p inhibits angiogenesis and inflammatory response in DR cell models via regulating CXCL8. BM-MSCs-derived exosomal miR-185-5p is expected to be the therapeutic target of DR.

Doi: <http://dx.doi.org/10.14715/cmb/2023.69.15.32>

Copyright: © 2023 by the C.M.B. Association. All rights reserved.

Introduction

At present, the incidence of diabetes is constantly increasing in China. As a kind of systemic metabolic disease, diabetes is easy to cause systemic complications (1). Diabetic retinopathy (DR) is the most common complication of patients' eyes. With the progression of diabetes, the incidence of DR is increasing. In addition, due to the irreversible course of DR, severe patients may even be blinded (2-4). Microangiopathy has been proven to be the pathological basis of DR (5, 6). Currently, the pathogenesis of DR is relatively complicated and has not been completely revealed. Therefore, the identification of molecules involved in angiogenesis and endothelial cell function can help to promote the therapeutic level of DR.

MicroRNA (miRNA) belongs to a type of non-coding molecule with around 22 nucleotides in length, which can post-transcriptionally modulate gene expression. Recently, a large body of miRNAs have been revealed to exert functions in diabetes together with associated complications, including DR (7, 8). Exosomes refer to small membrane vesicles (30-150 nm) including complex RNAs and proteins. Exosomes can be secreted by a variety of cells under normal and pathological conditions, and serum exosomes and osteoblast exosomes have been proven to affect tumors, Crohn's disease, osteopenia and other diseases by

secreting miRNAs (9-11). Additionally, literatures have revealed that miRNAs can be encapsulated in different types of exosomes to affect the progression of DR, and exosomal miRNAs have gradually become related diagnostic markers for diabetes and its complications (12). Retinal pigment epithelial cells have been found to secrete exosomes containing miR-202-5p to inhibit endothelium-mesenchymal transformation and fibrosis of DR, thus inhibiting the progression of proliferative DR (13).

MiR-185-5p has previously been shown to have decreased expression in diabetic macular edema (14). In addition, down-regulated expression of miR-185 has been also found in blood samples of diabetic patients, tissues and blood samples of diabetic rats (15). A major pathological feature of DR is retinal microvascular abnormality. Literatures have revealed that miR-185-5p can reduce RNCR3 and thus inhibit the excessive proliferation of retinal endothelial cells and retinal microvascular abnormality (16). In addition, the function of bone marrow-mesenchymal stem cells (BM-MSCs)-derived exosomal miR-185-5p in myocardial remodeling has been revealed, and the promotion of miR-185 expression can improve myocardial infarction (17). However, whether BM-MSCs-derived exosomal miR-185-5p affects DR remains to be further explored.

Interleukin-8 (IL-8), also named as CXC chemokine

* Corresponding author. Email: 20194133137@stu.suda.edu.cn

ligand 8 (CXCL8), is a cytokine in the chemokine family (18). Studies on proliferative DR have revealed that CXCL8 expression is enhanced in the vitreous body of patients with proliferative DR (19). In addition, CXCL8 is also an important target for increased expression of DR-associated angiogenic targets in retinal cells when palmitic acid and high-glucose (HG) are treated together in retinal cells (20). This study aimed to gain a new understanding of the regulation model of miR-185-5p on DR and develop a new molecular action pathway for DR treatment.

Materials and Methods

Bioinformatics analysis

The GEO chip expression data were obtained from the NCBI database, and the proliferative DR-related chip GSE60436 was selected. The GSE60436 chip contained the gene expression information of the fibrovascular membrane in 3 normal retina patients and 6 proliferative DR patients. GEO2R was implemented to analyze differentially expressed genes, and genetic screening conditions were set to adj. P.V al < 0.05 and | LogFoldChange | > 2. Compared with normal retina, the significantly up-regulated genes in proliferative DR were carried on GO enrichment analysis through online bioinformatics tools DAVID 6.8 database (<https://david.ncifcrf.gov/home.jsp>). The enrichment results of the first 20 channels with FDR (corrected P value) < 0.001 were selected for bubble mapping.

By virtue of the Venn online website (<http://bioinformatics.psb.ugent.be/webtools/Venn/>), a map of the intersection gene was drawn. Using the miRDB (<http://mirdb.org>) and StarBase (<http://starbase.sysu.edu.cn/>), the upstream target miRNAs of genes were obtained and the intersection was taken. DIANA TOOLS (<http://diana.imis.athenainnovation.gr/DianaTools/index.php?r=mirpath/index>) was implemented for the functional enrichment analysis of the intersection miRNAs.

Cell culture

Human retinal microvascular endothelial cells (HR-MECs) were purchased from Shanghai Jining Industrial Co., LTD. (China), and cultured in ECM medium (Sciencell, USA) including 5% fetal bovine serum (FBS) together with 1% growth factors at 37°C and 5% CO₂. Normal glucose (NG) group was added with 5.5 mmol/L glucose during culture. In addition, 30 mmol/L mannitol was added as the hyperosmolality control group. In the HG group, glucose was added to 30 mmol/L for 24 h, 48 h and 72 h.

Isolation and identification of exosomes from BM-MSCs

BM-MSCs were obtained from Shanghai Hongshun Biotechnology Co., LTD. (China), and the 3rd generation cell supernatant was taken and passed through a 0.22- μ m filter. Reagents of the ExoQuick TC Exosome Extraction

Kit (System Biosciences, USA) were mixed with the liquid phase of the cell supernatant, and the mixture was taken for centrifugation at 10000 \times g. The precipitation obtained after centrifugation was converted into exosomes according to the kit instructions. Exosome morphology was captured via transmission electron microscopy (Thermo Fisher, USA), and the expression of exosome markers CD63 together with TSG101 was examined by western blot.

2Cell transfection and grouping

well as miR-185-5p inhibitors were designed and obtained from RiboBio (Guangzhou, China). Exosomes and cells were transfected using the Exo-Fect transfection kit (System Biosciences, USA) and the Lipofectamine 3000 kit (Thermo Fisher, USA), respectively. The transfection sequence is shown in Table 1.

Dual-luciferase reporter gene assay

The bioinformatics online database miRDB and Starbase were implemented to predict the binding sequences between CXCL8 and miR-185-5p and the sequences were amplified. The report vectors of CXCL8 wild type (CXCL8-WT) and CXCL8 mutant type (CXCL8-MUT) were then constructed respectively. The miR-185-5p mimic and control mimic (miR-NC) obtained from Shanghai GenePharma Co., Ltd were transfected into cells using the Lipofectamine 3000 kit (Thermo Fisher, USA). Seventy-two hours after transfection, cells were rinsed with PBS, added with 250 μ L of 1 \times PLB lysate, centrifuged at 4000 \times g for 1 min, and the supernatant was taken for collection. The luciferase activity was assessed using a dual-luciferase reporter assay kit (Promega, USA). Firefly luciferase and sea kidney luciferase activities were adopted as relative luciferase activity detection values.

qRT-PCR detection of mRNA expression

Total RNA extraction was performed using TRIzol reagents (Invitrogen, USA), and RNA was taken for reverse transcription into complementary DNA (cDNA) by a RevertAid First Strand cDNA Synthesis Kit (Thermo Fisher, USA). Quantitative real-time PCR reactions were implemented on the ABI 7500 real-time PCR system (Applied Biosystems, USA) using PowerUP SYBR Green Master Mix (Thermo Fisher, USA). mRNA relative expression was measured by 2^{- $\Delta\Delta$ Ct}, and GAPDH was adopted as an internal reference. The sequence of primers used is displayed in Table 2.

Western blot detection of protein expression

RIPA lysis buffer (Shanghai Beyotime Biotechnology Co., LTD., China) was used to lyse cells on ice and a BCA protein quantification kit (Thermo Fisher, USA) was adopted to quantify the protein concentration. After gel electrophoresis, proteins were transferred to cellulose

Table 1. Transfection sequence.

pcDNA-NC	CATAGGACTGCGGCGATTGCCGTCCGA
pcDNA-CXCL8	TCAGCAGCTCACGCCTGGCTCGAACA
siRNA-NC	ACGTGCGACGCATGCTAGCAACGCC
siRNA-CXCL8	CGATGCGACGCTGCAGCGTGACGACG
inhibitor-NC	TGCAGCGACGCCGCTGCCAGCTAGCGCGTA
miR-185-5p inhibitor	ATGCGACGCTACGCAGCACGTACGAC

Table 2. qRT-PCR primer sequence.

Gene	Primer sequence (5'-3')
miR-185-5p	Forward: TGTCGTCTGGTTACTATATCTGCG
	Reverse: GCTGTACGAGCCATGCCCGTCA
CXCL8	Forward: CTAACCGTCGTCTGCGGTTCTAG
	Reverse: TGACGATCGTCTCTCGTTGAGTCT
GAPDH	Forward: ACTAGACGTGCATGTACTATTCC
	Reverse: AATGTCAGATGTCCTACCTACG
U6	Forward: CACTGTAGTCGCTAGCAATATGA
	Reverse: TAGCTAATCCCTACACGCTCCT

nitrate membranes (Invitrogen, USA). The membrane was sealed with 5% skim milk and then treated with primary antibody including CXCL8 (1/1000, ab289967, Abcam, UK), CD63 (1/1000, ab193349, Abcam, UK), TSG101 (1/2000, ab228013, Abcam, UK) and GAPDH (1/10000, ab181603, Abcam, UK). After washing with $1 \times$ TBST, the membrane was incubated further with secondary anti-goat anti-Rabbit IgG (1:1000, ab289875, Abcam, UK). The signal was examined using an enhanced chemiluminescence (ECL) kit (Abcam, UK), and the band strength was calculated using the software Image J (NIH, Bethesda, USA).

Angiogenesis experiment

A 96-well culture plate was precoated with Matrigel matrix gel (356234, Corning, USA), and then HRMECs (40000 cells/well) were inoculated to a 96-well culture plate for 24 h of culture, the angiogenesis was observed by means of DMILLED, Leica, Germany, and the vascular branches and length were measured via Image J software (NIH, Bethesda, USA).

Concentrations of VEGF and inflammatory factors using ELISA

The concentrations of VEGF, TNF- α , IL-1 β as well as IL-6 in the supernatant of each group were determined following the instructions (Hangzhou Lianke Biotechnology Co., LTD., China). The specific steps were as follows: The cells of each group were taken for centrifugation at the speed of $500 \times g$ for 5 min, and 100 μ L cell supernatant was added to each cell culture well, followed by the addition of 50 μ L antibody to be tested, and incubated at room temperature for 2 h after sealing. After rinsing with PBS, 100 μ L horseradish peroxidase-streptavidin was added into each well, followed by sealing and incubation at room temperature for 45 min. After rinsing with PBS, 100 μ L chromogenic substrate was taken to incubation in the dark for half an hour, and then 100 μ L termination solution was added. The absorbance at 450 nm was detected within 30 min.

Statistical analysis

All data were analyzed using GraphPad Prism 8 software. Data were expressed as mean \pm SD, and a comparison between both groups was performed by t-test. One-way ANOVA or two-way ANOVA was adopted for comparison among multiple groups. SNK-q test was used for pound-wise comparison of data between multiple groups, and Tukey was implemented as post hoc test. * $P < 0.05$ was statistically significant.

Results

Bioinformatics analysis results

Analysis of GSE60436 expression data showed a total of 571 significantly down-regulated genes together with 236 significantly up-regulated genes (Figure 1A). GO functional enrichment analysis was performed on 236 significantly up-regulated genes in DR through the DAVID database, and the bubble map was displayed in Figure 1B. Two genes, CXCL8 and THBS1, were identified by intersecting genes involved in the positive regulation of angiogenesis, immune response and inflammatory response (Figure 1C). The Disgenet website was used to find the top 10 risk genes for DR, the protein interaction of CXCL8, THBS1 and DR risk genes was analyzed through the String website, and the Cytoscape website was used for visualization, it was found that CXCL8 interacted more closely with DR risk genes than THBS1 (Figure 1D). Therefore, CXCL8 was selected for the next step of analysis.

CXCL8 expression is enhanced in HRMECs treated with HG

After treating HRMECs with normal glucose, mannitol and HG, CXCL8 expression in HRMECs of each group was detected. The results presented that relative to the

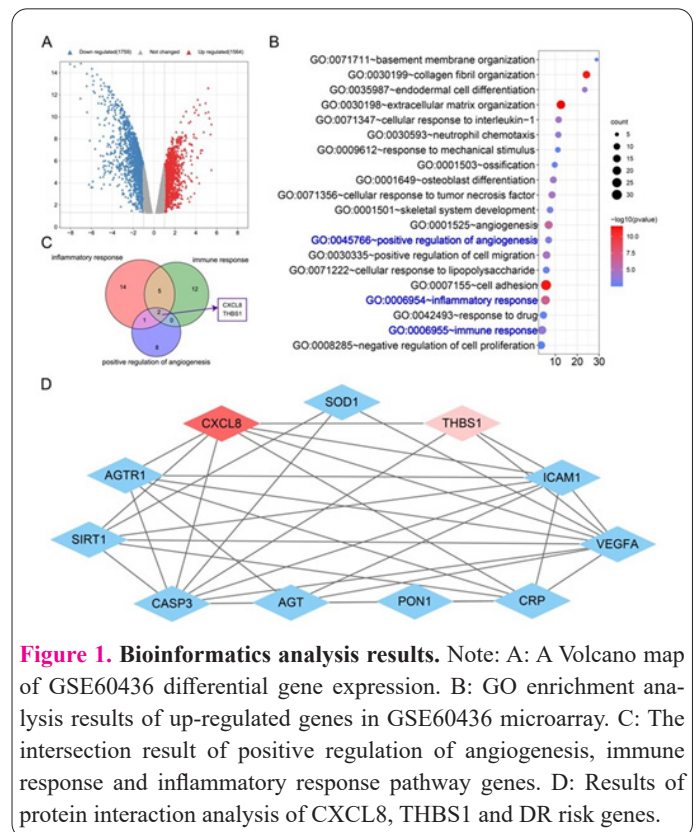


Figure 1. Bioinformatics analysis results. Note: A: A Volcano map of GSE60436 differential gene expression. B: GO enrichment analysis results of up-regulated genes in GSE60436 microarray. C: The intersection result of positive regulation of angiogenesis, immune response and inflammatory response pathway genes. D: Results of protein interaction analysis of CXCL8, THBS1 and DR risk genes.

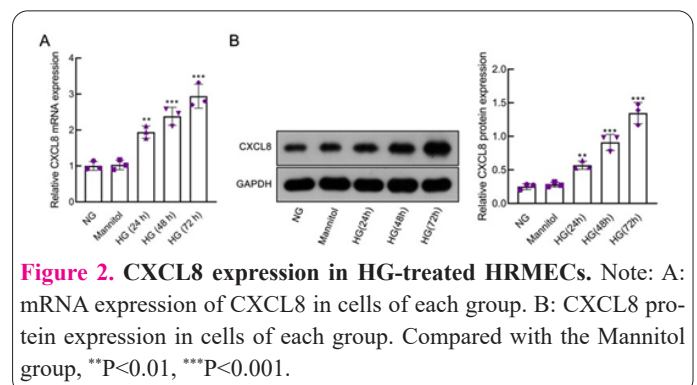


Figure 2. CXCL8 expression in HG-treated HRMECs. Note: A: mRNA expression of CXCL8 in cells of each group. B: CXCL8 protein expression in cells of each group. Compared with the Mannitol group, ** $P < 0.01$, *** $P < 0.001$.

mannitol group, CXCL8 expression in the HG group was gradually elevated with the extension of treatment time, as displayed in Figure 2.

CXCL8 affects angiogenesis and inflammatory response of HRMECs treated with HG

CXCL8 knockdown or overexpression was performed in HRMECs treated with HG. Figures 3A and 3B verified the knockdown and overexpression efficiency of CXCL8. In addition, CXCL8 overexpression enhanced the angiogenesis ability and increased the concentration of VEGF. Inversely, CXCL8 knockdown inhibited the angiogenesis and reduced VEGF concentration (Figure 3C-3D). The levels of inflammatory factors (TNF- α , IL-1 β and IL-6) were increased in the pcDNA-CXCL8 group, whereas levels of inflammatory factors (TNF- α , IL-1 β and IL-6) were inhibited in the siRNA-CXCL8 group (Figure 3E-3G).

Validation of upstream target miRNA of CXCL8

The upstream miRNAs of CXCL8 were analyzed by miRDB and Starbase, and a total of 8 intersection miRNAs were obtained (Figure 4A). The enrichment analysis of intersection miRNAs was performed by DIANA TOOLS, and it was found that miR-185-5p was enriched in more pathways (Figure 4B). ECM pathway and Hippo pathway have previously been confirmed to be related to DR, so miR-185-5p, which is enriched in both the Hippo pathway and the ECM receptor pathway, was selected for inclusion. The specific binding targets of CXCL8 and miR-185-5p were revealed in Figure 4C, and the targeted binding relationship between CXCL8 and miR-185-5p was further validated by the dual-luciferase reporter gene

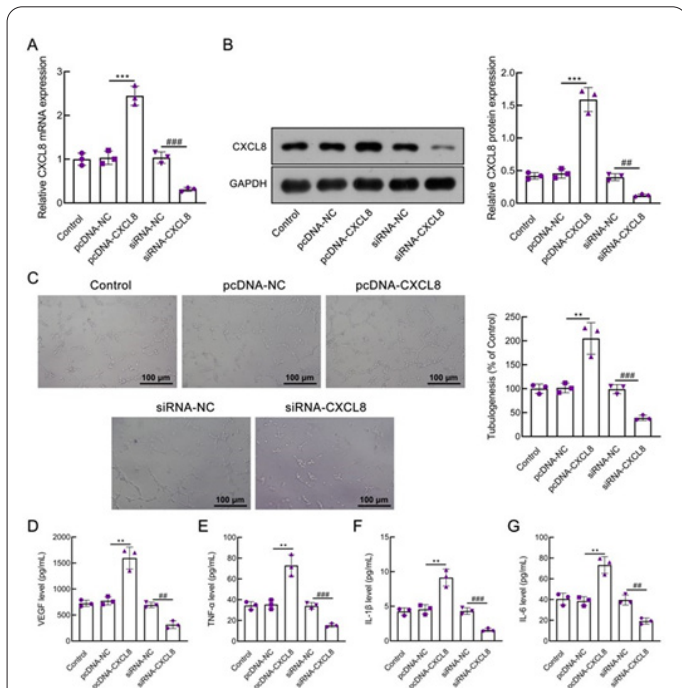


Figure 3. Impacts of CXCL8 on HRMECs treated with HG. Note: A: mRNA expression of CXCL8 in cells of each group. B: CXCL8 protein expression in each group. C: Detection results of angiogenesis in cells of each group (100 ×). D: Detection results of VEGF concentration in supernatant cells of each group. E-G: Detection results of the concentration of inflammatory factors in the cell supernatant of each group. Compared with pcDNA-NC group, **P<0.01, ***P<0.001; Compared with siRNA-NC group, ##P<0.01, ###P<0.001.

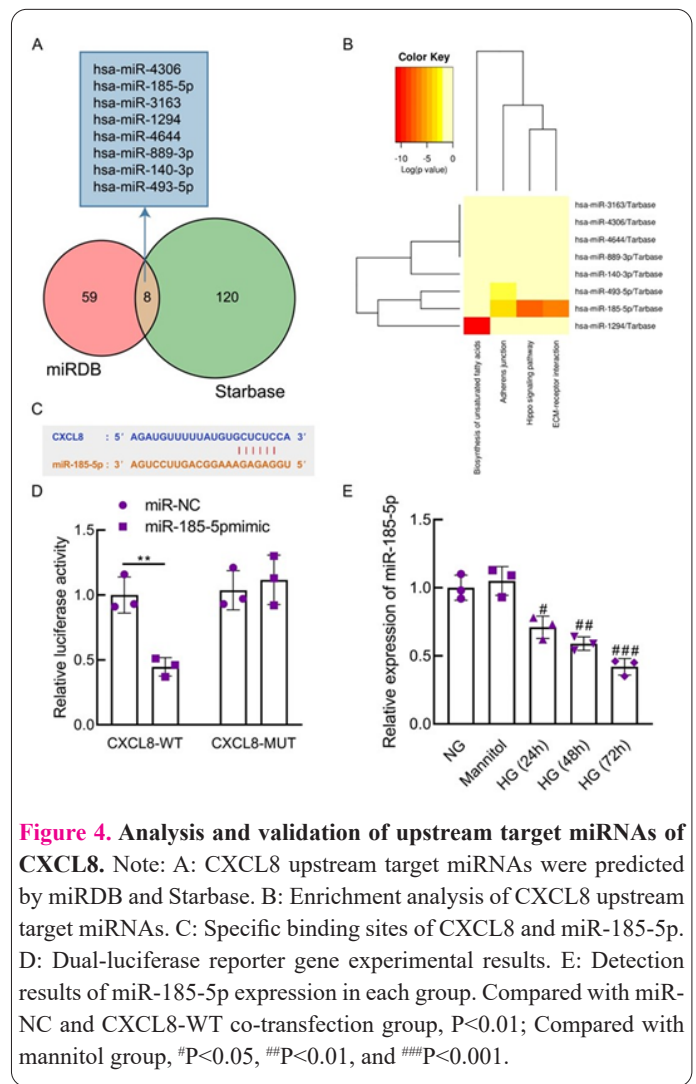


Figure 4. Analysis and validation of upstream target miRNAs of CXCL8. Note: A: CXCL8 upstream target miRNAs were predicted by miRDB and Starbase. B: Enrichment analysis of CXCL8 upstream target miRNAs. C: Specific binding sites of CXCL8 and miR-185-5p. D: Dual-luciferase reporter gene experimental results. E: Detection results of miR-185-5p expression in each group. Compared with miR-NC and CXCL8-WT co-transfection group, P<0.01; Compared with mannitol group, #P<0.05, ##P<0.01, and ###P<0.001.

experiment (Figure 4D). In addition, HRMECs treated with HG decreased miR-185-5p expression in a time-dependent manner with the increase in HG treatment time (Figure 4E).

BM-MSCs-derived exosomes inhibit angiogenesis and inflammatory response in HG-stimulated HRMECs

The exosomes of BM-MSCs were isolated and observed by projection electron microscopy. The exosomes exhibited a bilayer membrane vesicle structure (Figure 5A). The expressions of exosome markers CD63 and TSG101 in the BM-MSCs group were obviously increased (Figure 5B). The impacts of BM-MSCs-derived exosomes on angiogenesis and inflammatory response of HRMECs treated with HG were analyzed, and the results revealed (Figure 5C-5G) that, relative to the control group, the angiogenesis ability, concentration of VEGF and levels of inflammatory factors in BM-MSCs-Exos group were decreased.

The effect of BM-MSCs-derived exosomes on HRMECs treated with HG may be realized by mediating the expression of miR-185-5p/CXCL8

In order to probe whether the influence of BM-MSCs-derived exosomes on HRMECs treated with HG was related to miR-185-5p, miR-185-5p expression in BM-MSCs-Exos group was detected, and it was found that miR-185-5p expression was apparently enhanced in BM-MSCs-Exos group (Figure 6A). Additionally, the angiogenesis, concentration of VEGF, and levels of inflammatory

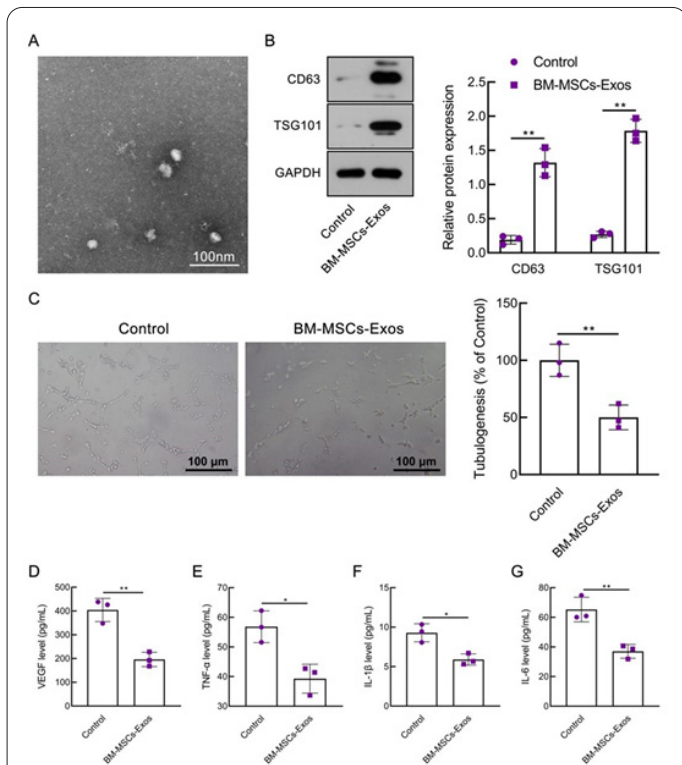


Figure 5. Effects of BM-MSCs-derived exosomes on angiogenesis and inflammatory response of HG treated HRMECs. Note: A: Electron microscopic observation of exosomes (40000 ×). B: Exosome marker detection results. C: Detection results of angiogenesis in cells of each group (100 ×). D: Detection results of VEGF concentration in supernatant cells of each group. E-G: The concentration of inflammatory factors in the cell supernatant of each group was detected. Compared with the Control group, *P<0.05 and **P<0.01.

cytokines in the BM-MSCs-Exos group were decreased. In addition, relative to the BM-MSCs-Exos+inhibitor-NC group, the angiogenesis, VEGF concentration and levels of inflammatory cytokines in the BM-MSCs-Exos+miR-185-5p inhibitor group were increased (Figure 6B-6F). It was suggested that BM-MSCs-derived exosomes affected the angiogenesis and inflammatory response of HRMECs by mediating miR-185-5p expression. Besides, it was found that CXCL8 expression in the BM-MSCs-Exos group was inhibited. Compared with the BM-MSCs-Exos+inhibitor-NC group, CXCL8 expression was enhanced in the BM-MSCs-Exos+miR-185-5p inhibitor group (Figure 6G-6H). Therefore, this study believed that the influence of BM-MSCs exosomes on HRMECs treated with HG might be realized by mediating miR-185-5p and CXCL8 expression.

Discussion

In this study, we focused on the influence and mechanism of BM-MSCs on the progression of DR by influencing angiogenesis and confirmed that BM-MSCs could secrete miR-185-5p and then inhibit DR angiogenesis and inflammatory response, while CXCL8 was also confirmed as the target of miR-185-5p and affected the progression of DR.

In this study, the differentially expressed genes related to DR were first analyzed with the help of the GEO database. After enrichment analysis of significantly up-regulated genes, angiogenesis, inflammatory response and other pathways were found. Considering that the pathological

basis of DR formation is microvascular disease, therefore, in this study, we chose to focus on the genes related to the angiogenic pathway, and after intersecting with other pathways, two genes were found in CXCL8 and THBS1. CXCL8 expression has previously been demonstrated to be significantly enhanced in the vitrectomy of DR patients, while CXCL8 expression was inhibited after vitrectomy (19). However, THBS1 was previously found to be inhibited in the preretinal fibrovascular membrane of proliferative DR patients (21), which was contrary to the results predicted by the chip. Therefore, CXCL8 in the chip was selected for research in this study. This study further demonstrated that CXCL8 expression was significantly up-regulated in HRMECs treated with HG, and functional experiments revealed that inhibition of CXCL8 expression could reduce the angiogenesis of HRMECs, the concentration of VEGF in cell supernatant and the level of inflammatory factors.

MiR-185-5p was found in the upstream target miRNAs of CXCL8, and further enrichment analysis exhibited that miR-185-5p was enriched in the ECM signaling pathway and Hippo signaling pathway. The ECM receptor pathway has been proven to be associated with DR (22). In addition, the Hippo pathway has also been proven to be one of the effective intervention pathways for diabetic retinopathy (23). In a study of diabetic macular edema, Cho H et al. discovered that miR-185-5p expression is reduced in patients with diabetic macular edema compared with heal-

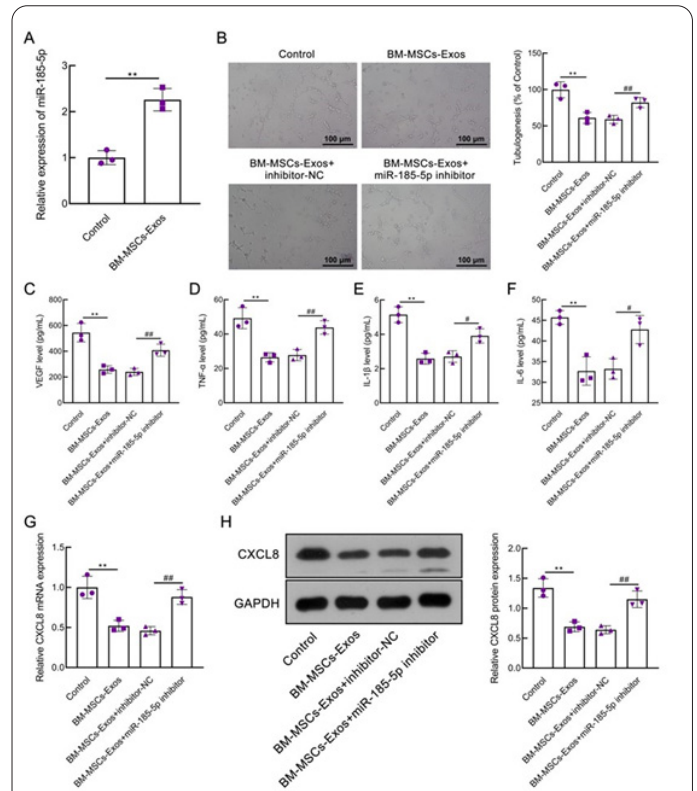


Figure 6. Expression of miR-185-5p/CXCL8 mediated by BM-MSCs exosomes affects HRMECs treated with HG. Note: A: miR-185-5p expression detection results. B: Detection results of angiogenesis in cells of each group (100×). C: Detection results of VEGF concentration in supernatant cells of each group. D-F: The concentration of inflammatory factors in the cell supernatant of each group was detected. G: Detection results of CXCL8 mRNA expression. H: Detection results of CXCL8 protein expression. Compared with the control group, **P<0.01. Compared with BM-MSCs-EXOs+inhibitor-NC group, #P<0.05 and ##P<0.01.

thy controls [14]. RNCR3 has been confirmed as a key regulatory factor of microvascular disorders of DR, and miR-185-5p can inhibit RNCR3 expression and thus delay the progression of DR (16). This study further revealed the relation between miR-185-5p and CXCL8.

As a type of pluripotent stem cells, BM-MSCs are capable of multi-differentiation and self-renewal. A number of reports have pointed out that BM-MSCs play a role in many diseases, such as kidney disease (24), osteogenesis induction and bone repair (25), tumors (26), rheumatoid arthritis (27), and heart-related diseases (28). In addition, it has been documented that BM-MSCs play a protective role in DR. Zhao H et al have manifested that BM-MSCs can inhibit the progression of DR by inhibiting oxidative stress and inflammatory pathways (29). Another study has shown that BM-MSCs exosomes can secrete miR-486-3p, thereby affecting apoptosis and inflammatory response of retinal endothelial cells, thus achieving the regulatory effect on DR (30). Besides, BM-MSCs have been proved to have a protective role in DR by affecting the Wnt pathway transduction and angiogenesis (31). This study previously revealed that miR-185-5p expression was decreased in DR, and later confirmed the protective effect of BM-MSCs in DR. Previous studies on myocardial infarction have shown that BM-MSCs exosomes can improve ventricular remodeling in mice with myocardial infarction by secreting miR-185 (17). In order to further verify the way that BM-MSCs play a role in DR, this study detected miR-185-5p expression in the exosomes derived by BM-MSCs and confirmed that miR-185-5p expression was elevated in the exosomes derived by BM-MSCs. Functional experiments confirmed that BM-MSCs-derived exosomes play a protective role in DR through modulating miR-185-5p expression.

In summary, this study verified that the BM-MSCs-derived exosomal miR-185-5p improved the angiogenesis and inflammatory response of DR by inhibiting CXCL8 expression (Figure 7). Of course, the conclusions of this study still need to be further verified. The limitation of this study is that due to the influence of funding, no *in vivo* experiments are conducted for further verification, and other factors affecting DR such as oxidative stress and apoptosis are not explored. In addition, no further researches are done on the downstream effects of CXCL8 or the signaling pathway, which is what we will work on later.

Ethical approval

No applicable.

Consent to publish

All authors gave final approval of the version to be published.

Conflicts of interest

The authors report no conflict of interest.

Author contributions

Weixia Wang conceived and designed the project, and wrote the paper, Lin Zhou generated and analyzed the data, and modified the manuscript. All authors gave final approval of the version to be published, and agreed to be accountable for all aspects of the work.

Availability of data and materials

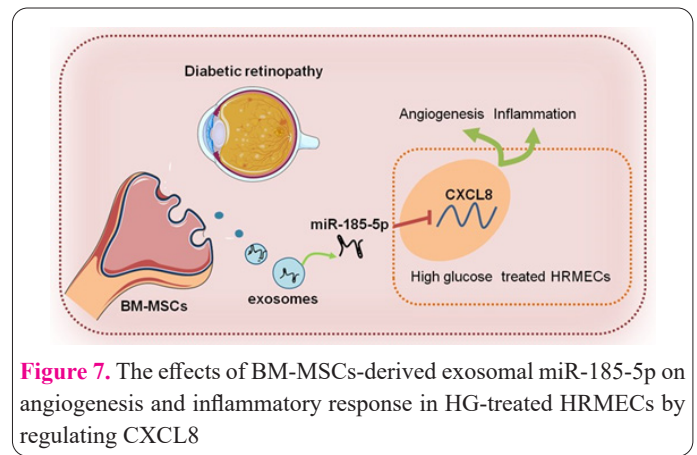


Figure 7. The effects of BM-MSCs-derived exosomal miR-185-5p on angiogenesis and inflammatory response in HG-treated HRMECs by regulating CXCL8

The data that support the findings of this study are available from the corresponding author upon reasonable request.

Funding

Not applicable.

Acknowledgements

Not applicable.

References

1. Wu LT, Wang JL, Wang YL. Ophthalmic artery changes in type 2 diabetes with and without acute coronary syndrome. *J Transl Med* 2022;20(1):512. doi: 10.1186/s12967-022-03712-0.
2. Sun J, Liu G, Chen R, Zhou J, Chen T, Cheng Y, et al. PARP1 Is Upregulated by Hyperglycemia Via N6-methyladenosine Modification and Promotes Diabetic Retinopathy. *Discov Med* 2022;34(172):115-29. doi:
3. Lee YJ, Jeon HY, Lee AJ, Kim M, Ha KS. Dopamine ameliorates hyperglycemic memory-induced microvascular dysfunction in diabetic retinopathy. *Faseb j* 2022;36(12):e22643. doi: 10.1096/fj.202200865R.
4. Yang S, Guo X, Cheng W, Seth I, Bulloch G, Chen Y, et al. Genome-wide DNA methylation analysis of extreme phenotypes in the identification of novel epigenetic modifications in diabetic retinopathy. *Clin Epigenetics* 2022;14(1):137. doi: 10.1186/s13148-022-01354-z.
5. Han R, Jin M, Xu G, He J. Progressively Decreased HCN1 Channels Results in Cone Morphological Defects in Diabetic Retinopathy. *J Neurosci* 2022;42(43):8200-12. doi: 10.1523/jneurosci.2550-21.2022.
6. Gong R, Han R, Zhuang X, Tang W, Xu G, Zhang L, et al. MiR-375 mitigates retinal angiogenesis by depressing the JAK2/STAT3 pathway. *Aging (Albany NY)* 2022;14(16):6594-604. doi: 10.18632/aging.204232.
7. Beuzelin D, Kaeffer B. Exosomes and miRNA-Loaded Biomimetic Nanovehicles, a Focus on Their Potentials Preventing Type-2 Diabetes Linked to Metabolic Syndrome. *Front Immunol* 2018;9:2711. doi: 10.3389/fimmu.2018.02711.
8. Platania CBM, Maisto R, Trotta MC, D'Amico M, Rossi S, Gesualdo C, et al. Retinal and circulating miRNA expression patterns in diabetic retinopathy: An *in silico* and *in vivo* approach. *Br J Pharmacol* 2019;176(13):2179-94. doi: 10.1111/bph.14665.
9. Kahroba H, Samadi N, Mostafazadeh M, Hejazi MS, Sadeghi MR, Hashemzadeh S, et al. Evaluating the presence of deregulated tumoral onco-microRNAs in serum-derived exosomes of gastric cancer patients as noninvasive diagnostic biomarkers. *Bioimpacts* 2022;12(2):127-38. doi: 10.34172/bi.2021.22178.
10. Chen P, Huang S, Yu Q, Chao K, Wang Y, Zhou G, et al. Serum

- exosomal microRNA-144-3p: a promising biomarker for monitoring Crohn's disease. *Gastroenterol Rep (Oxf)* 2022;10:goab056. doi: 10.1093/gastro/goab056.
11. Hu CH, Sui BD, Liu J, Dang L, Chen J, Zheng CX, et al. Sympathetic Neurostress Drives Osteoblastic Exosomal MiR-21 Transfer to Disrupt Bone Homeostasis and Promote Osteopenia. *Small Methods* 2022;6(3):e2100763. doi: 10.1002/smt.202100763.
 12. He X, Kuang G, Wu Y, Ou C. Emerging roles of exosomal miRNAs in diabetes mellitus. *Clin Transl Med* 2021;11(6):e468. doi: 10.1002/ctm.2.468.
 13. Gu S, Liu Y, Zou J, Wang W, Wei T, Wang X, et al. Retinal pigment epithelial cells secrete miR-202-5p-containing exosomes to protect against proliferative diabetic retinopathy. *Exp Eye Res* 2020;201:108271. doi: 10.1016/j.exer.2020.108271.
 14. Cho H, Hwang M, Hong EH, Yu H, Park HH, Koh SH, et al. Micro-RNAs in the aqueous humour of patients with diabetic macular oedema. *Clin Exp Ophthalmol* 2020;48(5):624-35. doi: 10.1111/ceo.13750.
 15. Zhao Y, Guo L, Tian J, Wang H. Downregulation of microRNA-185 expression in diabetic patients increases the expression of NOS2 and results in vascular injury. *Exp Ther Med* 2021;22(6):1458. doi: 10.3892/etm.2021.10893.
 16. Shan K, Li CP, Liu C, Liu X, Yan B. RNCR3: A regulator of diabetes mellitus-related retinal microvascular dysfunction. *Biochem Biophys Res Commun* 2017;482(4):777-83. doi: 10.1016/j.bbrc.2016.11.110.
 17. Li Y, Zhou J, Zhang O, Wu X, Guan X, Xue Y, et al. Bone marrow mesenchymal stem cells-derived exosomal microRNA-185 represses ventricular remodeling of mice with myocardial infarction by inhibiting SOCS2. *Int Immunopharmacol* 2020;80:106156. doi: 10.1016/j.intimp.2019.106156.
 18. Middleton FM, McGregor R, Webb RH, Wilson NJ, Moreland NJ. Cytokine imbalance in acute rheumatic fever and rheumatic heart disease: Mechanisms and therapeutic implications. *Autoimmun Rev* 2022;21(12):103209. doi: 10.1016/j.autrev.2022.103209.
 19. Yoshida S, Kubo Y, Kobayashi Y, Zhou Y, Nakama T, Yamaguchi M, et al. Increased vitreous concentrations of MCP-1 and IL-6 after vitrectomy in patients with proliferative diabetic retinopathy: possible association with postoperative macular oedema. *Br J Ophthalmol* 2015;99(7):960-6. doi: 10.1136/bjophthalmol-2014-306366.
 20. Capozzi ME, Giblin MJ, Penn JS. Palmitic Acid Induces Müller Cell Inflammation that is Potentiated by Co-treatment with Glucose. *Sci Rep* 2018;8(1):5459. doi: 10.1038/s41598-018-23601-1.
 21. Kim LA, Wong LL, Amarnani DS, Bigger-Allen AA, Hu Y, Marko CK, et al. Characterization of cells from patient-derived fibrovascular membranes in proliferative diabetic retinopathy. *Mol Vis* 2015;21:673-87. doi: 10.1016/j.molvis.2015.06.011.
 22. Xie T, Chen X, Chen W, Huang S, Peng X, Tian L, et al. Curcumin is a Potential Adjuvant to Alleviates Diabetic Retinal Injury via Reducing Oxidative Stress and Maintaining Nrf2 Pathway Homeostasis. *Front Pharmacol* 2021;12:796565. doi: 10.3389/fphar.2021.796565.
 23. Hao GM, Lv TT, Wu Y, Wang HL, Xing W, Wang Y, et al. The Hippo signaling pathway: a potential therapeutic target is reversed by a Chinese patent drug in rats with diabetic retinopathy. *BMC Complement Altern Med* 2017;17(1):187. doi: 10.1186/s12906-017-1678-3.
 24. Xu S, Cheuk YC, Jia Y, Chen T, Chen J, Luo Y, et al. Bone marrow mesenchymal stem cell-derived exosomal miR-21a-5p alleviates renal fibrosis by attenuating glycolysis by targeting PFKM. *Cell Death Dis* 2022;13(10):876. doi: 10.1038/s41419-022-05305-7.
 25. Yu K, Huangfu H, Qin Q, Zhang Y, Gu X, Liu X, et al. Application of Bone Marrow-Derived Macrophages Combined with Bone Mesenchymal Stem Cells in Dual-Channel Three-Dimensional Bioprinting Scaffolds for Early Immune Regulation and Osteogenic Induction in Rat Calvarial Defects. *ACS Appl Mater Interfaces* 2022;14(41):47052-65. doi: 10.1021/acsami.2c13557.
 26. Yu T, Yu H, Xiao D, Cui X. Human Bone Marrow Mesenchymal Stem Cell (hBMSCs)-Derived miR-29a-3p-Containing Exosomes Impede Laryngocarcinoma Cell Malignant Phenotypes by Inhibiting PTEN. *Stem Cells Int* 2022;2022:8133632. doi: 10.1155/2022/8133632.
 27. Jung N, Park S, Kong T, Park H, Seo WM, Lee S, et al. LC-MS/MS-based serum proteomics reveals a distinctive signature in a rheumatoid arthritis mouse model after treatment with mesenchymal stem cells. *PLoS One* 2022;17(11):e0277218. doi: 10.1371/journal.pone.0277218.
 28. Qiu J, Xiao H, Zhou S, Du W, Mu X, Shi G, et al. Bone marrow mesenchymal stem cells inhibit cardiac hypertrophy by enhancing FoxO1 transcription. *Cell Biol Int* 2021;45(1):188-97. doi: 10.1002/cbin.11482.
 29. Zhao H, He Y. Lysophosphatidylcholine Offsets the Protective Effects of Bone Marrow Mesenchymal Stem Cells on Inflammatory Response and Oxidative Stress Injury of Retinal Endothelial Cells via TLR4/NF- κ B Signaling. *J Immunol Res* 2021;2021:2389029. doi: 10.1155/2021/2389029.
 30. Li W, Jin L, Cui Y, Nie A, Xie N, Liang G. Bone marrow mesenchymal stem cells-induced exosomal microRNA-486-3p protects against diabetic retinopathy through TLR4/NF- κ B axis repression. *J Endocrinol Invest* 2021;44(6):1193-207. doi: 10.1007/s40618-020-01405-3.
 31. Ebrahim N, El-Halim HEA, Helal OK, El-Azab NE, Badr OAM, Hassouna A, et al. Effect of bone marrow mesenchymal stem cells-derived exosomes on diabetes-induced retinal injury: Implication of Wnt/ b-catenin signaling pathway. *Biomed Pharmacother* 2022;154:113554. doi: 10.1016/j.biopha.2022.113554.